Hindawi
International Journal of Aerospace Engineering
Volume 2018, Article ID 9724263, 15 pages
https://doi.org/10.1155/2018/9724263

Research Article

Design, Analysis, Optimization, Manufacturing, and Testing of a 2U Cubesat

Andreas Ampatzoglou and Vassilis Kostopoulos

Applied Mechanics Laboratory, Mechanical Engineering and Aeronautics Department, University of Patras, Rio Campus, 26500 Patras, Greece

Correspondence should be addressed to Vassilis Kostopoulos; kostopoulos@upatras.gr

Received 24 October 2017; Revised 21 February 2018; Accepted 25 March 2018; Published 12 June 2018

Academic Editor: Vaios Lappas

The design optimization, development, and verification by analysis and testing of the 1st Greek cubesat, developed by the University of Patras and Libre Space Foundation (UPSat (University of Patras Satellite)), is presented. The key innovative approach includes the replacement of the aluminum side faces with structural composite components, keeping the commonly used aluminum frame. A "hybrid" double-unit (2U) cubesat structure was optimized, built, and tested for all launch and thermal loads/specifications required for launch and mission operations as imposed from the EU-funded FP7-QB50 project. Results show that the new design of the structure using CFRP can offer similar levels of performance in terms of stiffness, while saving 30% of the mass, for the entire cubesat platform.

1. Introduction

In the last few decades, a fast-growing small satellite industry has enabled increasingly capable and cost-effective space missions, by embracing reduced requirements and integrating commercial technology. Academic research has been active in this field for many years and has resulted in the development of nanosatellites (<10 kg) and picosatellites (<1 kg) with an emphasis on decreasing the platform size through application of advanced technologies. In this framework, California Polytechnic State University (CalPoly) and Stanford University's Space Systems Development Laboratory developed the cubesat program and published a standard [1] that specifies major requirements and constrains as well as important guidelines that each cubesat must deal with as the design progresses.

As for all space missions, including cubesats, the structure is one of the main satellite subsystems. In principle, the purpose of the structural subsystem is to provide a simple and robust structure that shall survive launch loads and provide a suitable environment for the operation of all subsystems. Furthermore, the structure mechanically supports all other spacecraft subsystems, attaches the spacecraft to the launch vehicle, and provides for ordnance-activated separation [2]. Generally, structural design shall aim for simple load paths, simplified interfaces, and easy integration.

The design of space structural systems is dictated by mass, stiffness, and strength requirements. On the one hand, stiffness is required to ensure the survivability of the instrumentation; on the other hand, by reducing the weight, it is possible to increase the payload, which extends the mission goals and also reduces the launch cost [3]. The structural and mechanical parts of a satellite generally represent a large percentage of its mass, and therefore, it is important to choose the proper material [4] and structural configuration to minimize mass. Finally, cubesat design is bound by the general constrains and requirements of stiffness and principal eigenfrequency [5].

Until now, numerous cubesat missions have successfully been launched. An extensive survey of current cubesat missions and their capabilities can be found in [6, 7]. The primary choice for structural systems is aluminum alloys

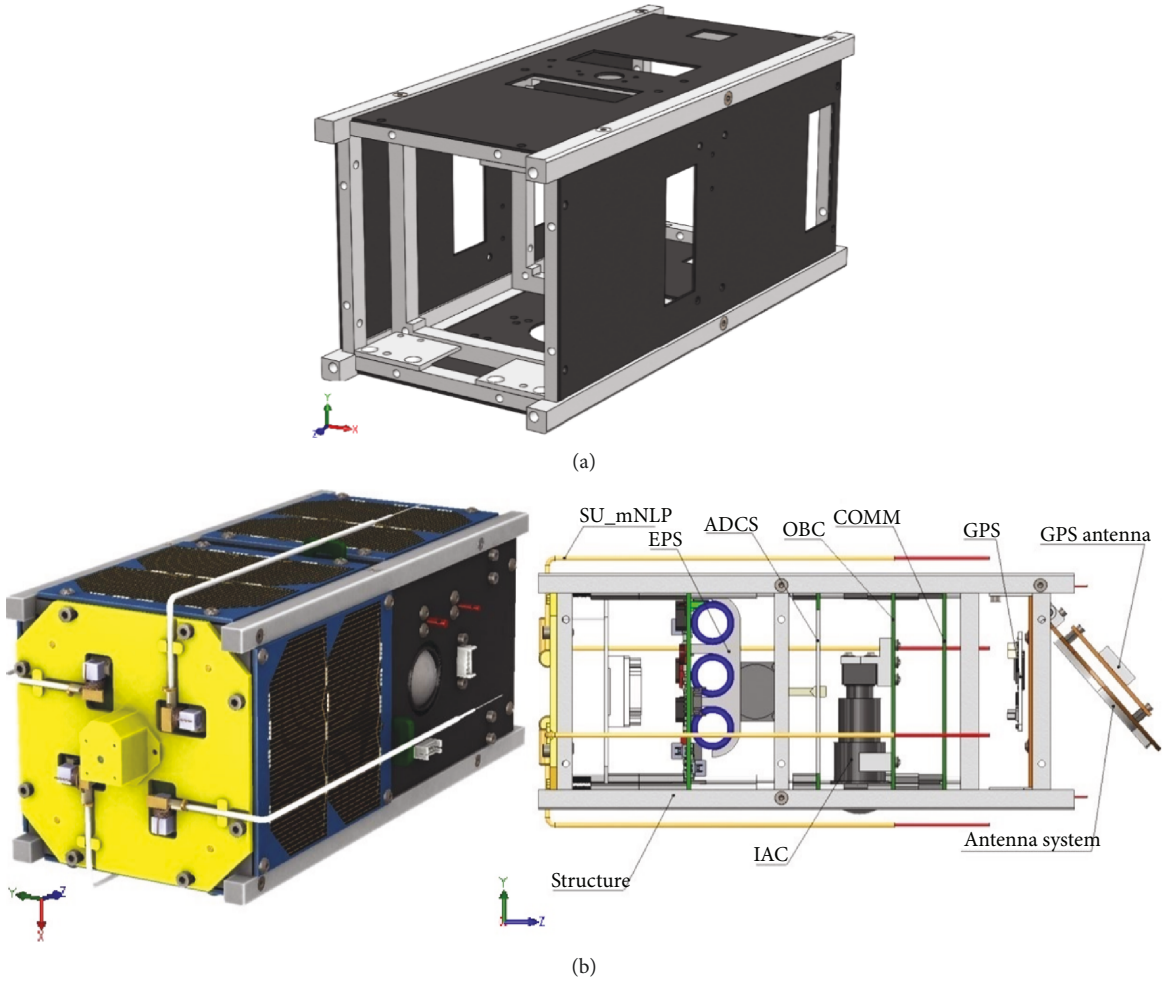

Figure 1: CAD design for the "hybrid" structure (a) and the fully assembled cubesat (b).

with the most common being 6061 or 7075 and respective grades, materials that meet the requirement of having thermal expansion factors equal to the Poly Picosat Orbital Deployer (P-POD) material [1].

The current work focuses on the design, verification by analysis, and test of a 2U cubesat for a specific LEO (low Earth orbit) mission (FP7-QB50 project) and also on the investigation of the use of CFRP (carbon fiber reinforced plastic) materials in space structural design. Their application has advantages concerning mass and strength, and the required stiffness can be achieved by an appropriate choice of fiber types and orientation in a laminate [8].

Given the mass, stiffness, and strength requirements of the spacecraft and the interfaces to the separation module, we attempt to design and prove the feasibility of designing and qualifying a cubesat structure made of both composite materials and aluminum alloy. The structure design follows the commonly used scenario of an aluminum frame, and all side faces were replaced with CFRP parts. Both the finite element analysis (FEA) and testing campaigns included all the launch loads according to cubesat and QB50 specifications and concluded successfully.

Table 1: Material properties.

(a)

HTM143/M55J properties	
E11 (GPa)	181
E2 (GPa)	10.3
G12 (GPa)	7.17
v12	0.28
G13 (GPa)	3.38
ρc (kg/m3)	1600

(b)

	Alum. alloy 7075 properties	St. steel properties
E (GPa)	71.7	200
v	0.33	0.33
ρ (kg/m3)	2710	7800

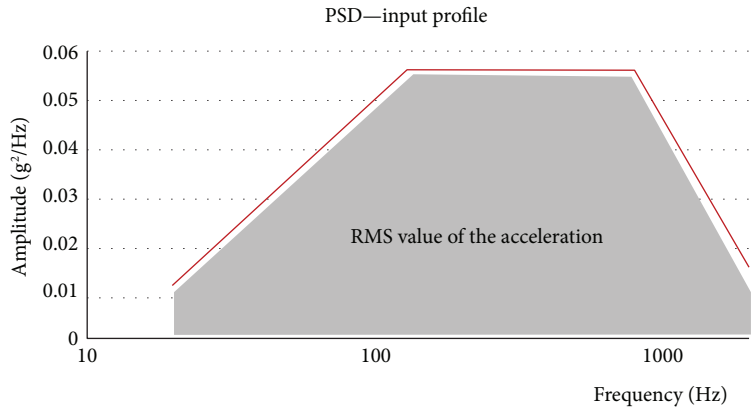

Figure 2: Frequency (Hz) versus amplitude (g^2/Hz) chart (QB50 mission).

2. Cubesat Structure Design and Modelling

2.1. Cubesat Structural Design. The design process of the structure is an iterative process as is the case with the other subsystems. The process accounts for the upcoming necessary changes evolving from the interaction between the subsystems [9]. In the previous work [10], a comparison between a full composite 1U structure and cubesat-kit design in terms of mass and stiffness took place, showing that considering the proper lamination for the composite structure, the 1st eigenfrequency of the structure was increased and at the same time, a significant mass reduction was achieved (close to 35%). Furthermore, using CFRP as the primary structural component, the structural behavior at launch loads (quasistatic and random vibration) is improving, in terms of the maximum stresses and displacements developed.

Having as baseline the design for the 1U UPSat [11], the lamination of the composite parts, and the QB50 Design Requirements [11], the optimized "hybrid" structure presented in Figure 1 was designed. This design was based on an aluminum frame, giving ease of access in the internal, with all side faces bolted together. For the UPSat scenario, the side faces are four; the +Z face must be available for accommodating a Science Unit and the −Z face for accommodating the antenna system.

The assembly was realized in two different ways: one using solid bodies for all parts for visualization reasons and one using surfaces for the CFRP components and all electronic components. The surface assembly was created for the finite element analysis, so meshing could be done with shell elements. This was feasible because of the small thickness-to-length (0.004) ratio and thickness-to-width (0.011) ratio of each structural component and also for creating a more simplified finite element model. A shell element finite element model is not time consuming regarding both the building process of the model and the analysis run time.

The design was realized in such a way that all the necessary subsystems for a cubesat mission are included in the analysis. These components/subsystems were designed from scratch and included the electronic equipment (PCBs (printed circuit board)), solar panels on the external faces, a

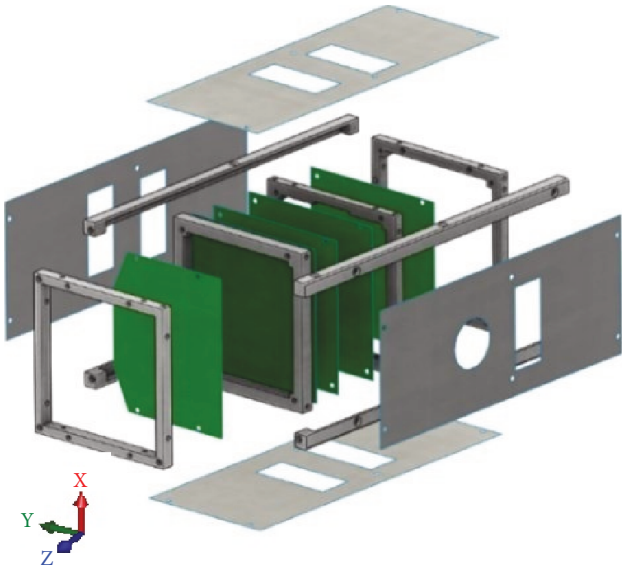

Figure 3: CAD design using surfaces and solid parts.

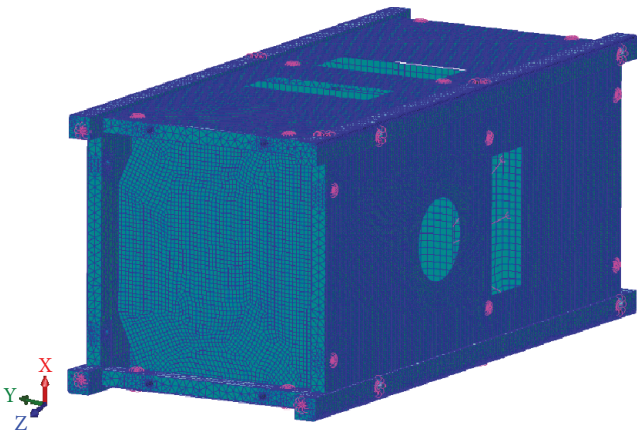

Figure 4: Finite element model.

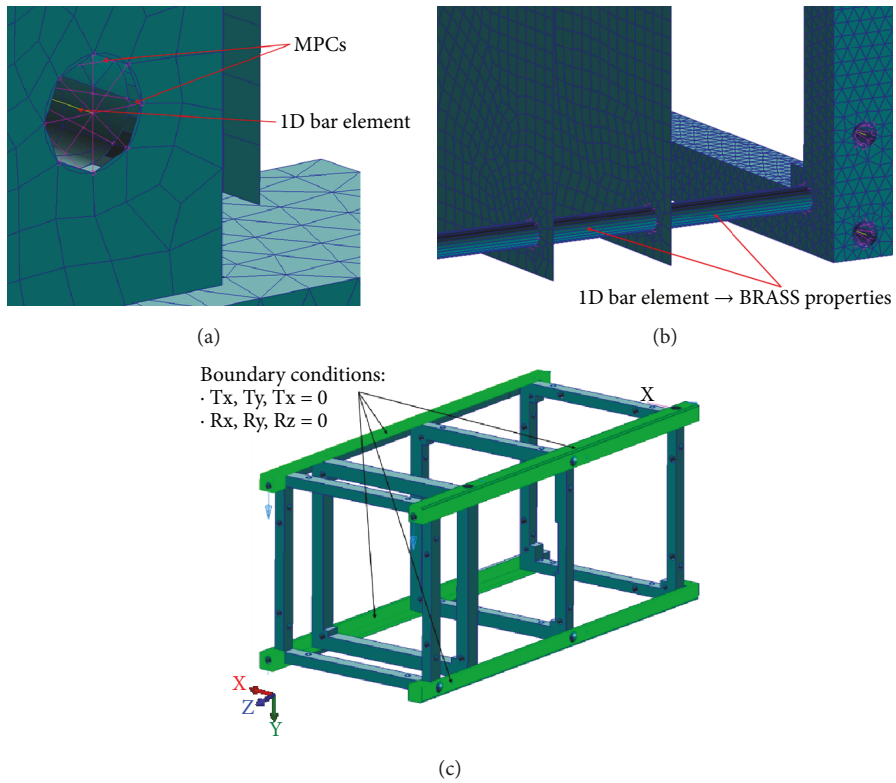

Figure 5: (a) Bolted connections, (b) inner structure, and (c) boundary conditions.

Table 2: FR4 properties.

ρ (kg/m^3)	1850
E (GPa)	22
v	0.136

camera, and the antenna system on the −Z face. For PCB mounting, the commonly used solution of spacers was followed, and all PCBs along with the spacers were modelled during the finite element analysis campaign. On the +Z face, a Science Unit was attached (provided by von Karman Institute, QB50 project coordinator).

2.2. Cubesat Structure Materials. A space-approved composite material, namely, HTM143/M55J (6K) Cyanate-Ester/Carbon unidirectional pre-preg made by CYTEC, was selected for the present application. Table 1 shows the necessary set of properties of the pre-preg material considered during finite element modeling. After a trade-off study considering stiffness and mass requirements [10], a quasi-isotropic lay-up was concluded. The resulting lay-up is [0/45/90/−45] S, an eight-layer lay-up which ends up to a total thickness of 1 mm. This lay-up was considered for all side faces of the cubesat.

All aluminum components were made of 7075 aluminum alloy (T6), one of the two most commonly used aluminum alloys for such applications (the second one is the 6061 alloy). The properties of aluminum alloy 7075 used in the analysis are also given in Table 1. Finally, all bolts used for the connection of the different components considered to be made of stainless steel and the relevant properties used are given in Table 1.

A preliminary calculation took place inside the SolidWorks environment considering the mass saving from the replacement of the aluminum sides with composite parts. The total mass of four components was calculated to be 133 grams with the use of a composite material and 227 grams using aluminum alloy. This 94 grams is equivalent to a mass reduction close to 40% and used for extra scientific equipment for fulfilling the mission's objectives.

2.3. Launch Environment and Analysis Scenarios. A typical cubesat device will be launched on a variety of launching rockets. To qualify for acceptance, the cubesat structure must not fail under certain static and dynamic loading that will be calculated based on the launching conditions. The launching rocket puts out random excitation, and for avoiding channeling this energy into violent resonance of the structure, the first frequency of free vibration should be above 70–90 Hz.

Thus, based on current qualification by analysis procedures [12], all launch loading scenarios required by QB50 mission were considered: a modal analysis, a quasistatic analysis, and the random vibration (PSD) analysis. The specific details of each are given hereafter. In addition, considering the thermal loads during cubesat operation in low Earth orbit, a thermal analysis is also conducted.

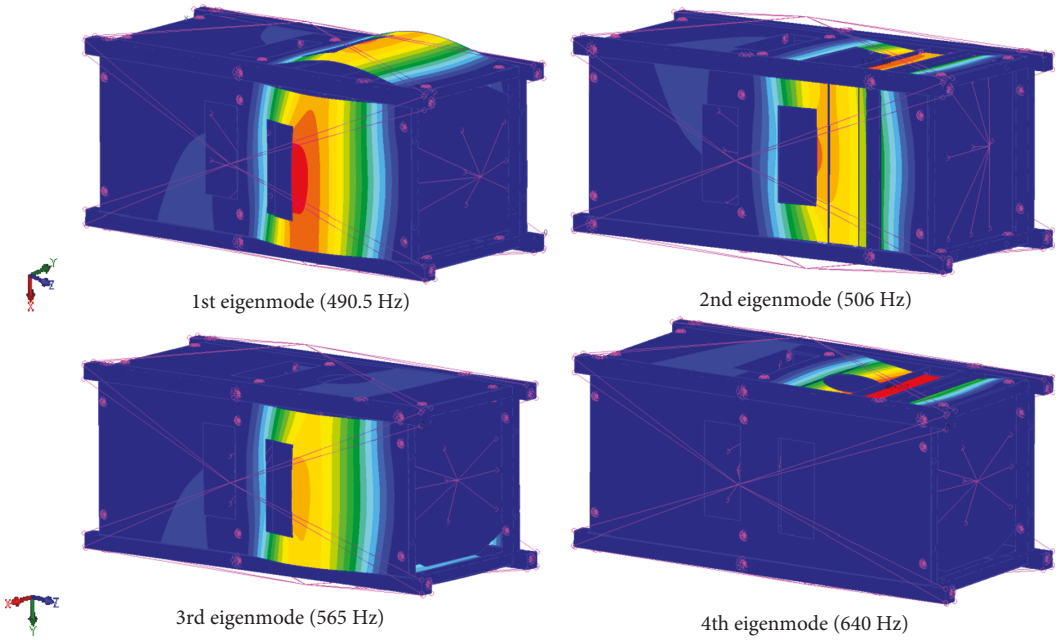

Figure 6: The first 4 eigenfrequencies and mode shapes for "hybrid" UPSat.

Table 3: Quasistatic analysis results.

	x-axis	y-axis	z-axis
Displacement (mm)	0.031	0.034	0.00372
STRESS—CFRP *(max principal)* (MPa)	6.95	6.55	1.18
STRESS—ALUM *(von Mises)* (MPa)	15.2	11.6	25.6
STRESS—PCBs (MPa)	4.4	4.7	2.06
STRESS—spacers (MPa)	3.8	4	1.5
STRAIN	$6.73 * 10^{-5}$	$6.89 * 10^{-5}$	$7.39 * 10^{-6}$

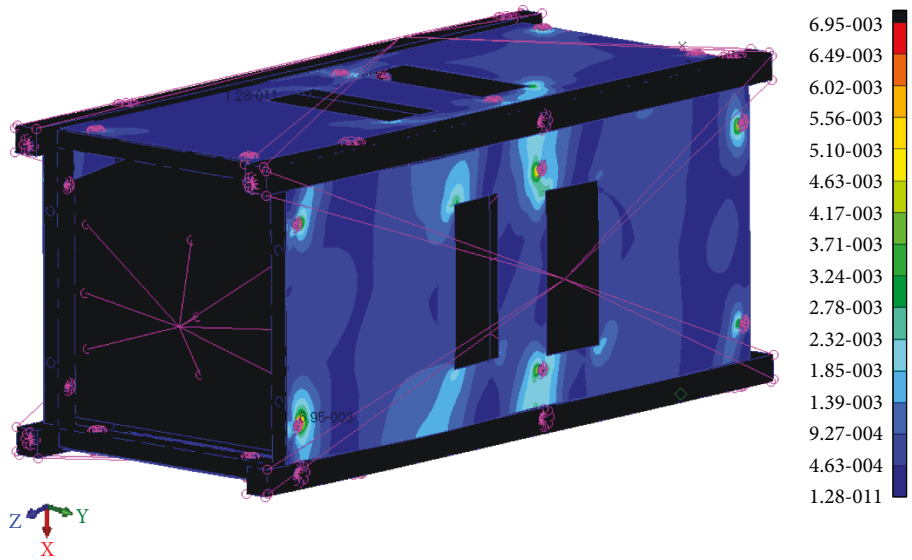

Figure 7: Stress distribution (x-axis).

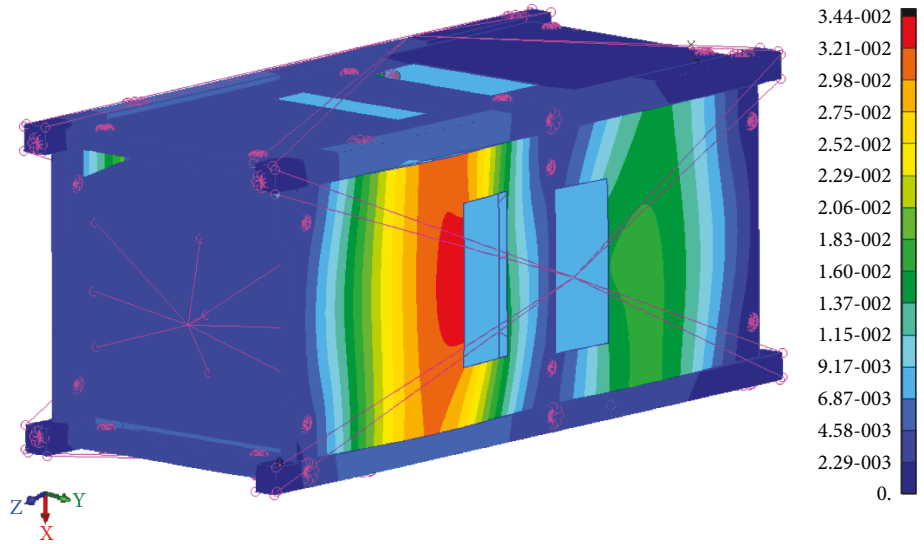

Figure 8: Displacement distribution (x-axis).

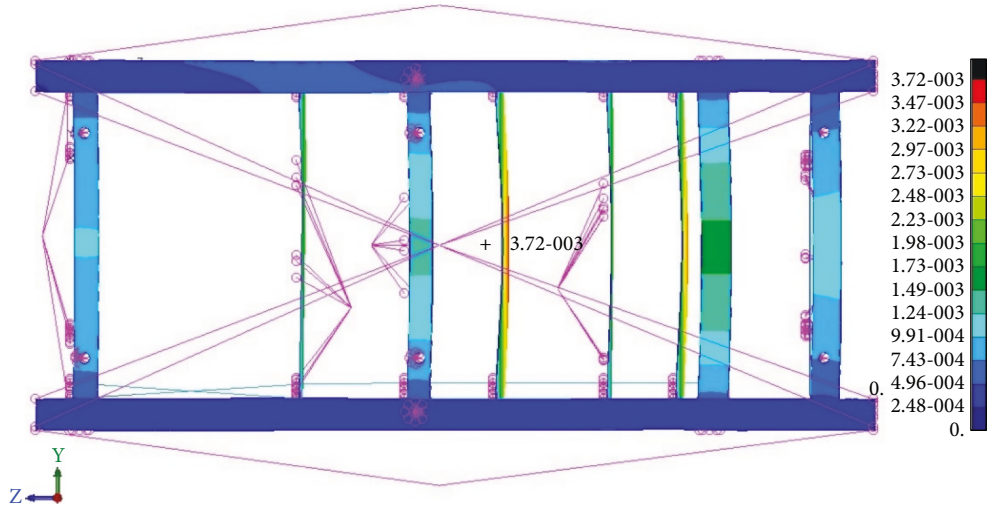

Figure 9: Stress distribution (z-axis).

2.3.1. Modal Analysis. The first step during a dynamic analysis is the determination of natural frequencies (eigenfrequencies) and mode shapes of structure, considering zero damping. The results of this analysis characterize the dynamic behavior of the structure and can show how the structure will respond under dynamic loads [13]. The most important modal characteristic of a space structure, like the cubesat, is the natural frequency threshold—meaning that the first natural frequency of the structure must be above a specific value, which usually is determined by the launch vehicle. The typical range for such missions is between 50 and 90 Hz.

At first, a modal analysis of the system under free-free boundary conditions is performed. This is done as an intermediate verification step for the connectivity of developed FE models. Then, the boundary conditions of the P-POD are applied, and another modal analysis is performed. This part shall reveal the real case scenario of the structural system.

2.3.2. Quasistatic Analysis. During the second scenario, the extreme quasistatic loading conditions of a cubesat were identified. The quasistatic event is loads that are independent of time or vary slowly, so that the dynamic response of the structure is not significant. In this base, for design purposes, the quasistatic loads are normally calculated by combining both static and dynamic load contributions. In this context, the quasistatic loads are equivalent to static loads, typically expressed as equivalent accelerations at the CoG [14].

The maximum amplitude of these loads is generally encountered at the end of the first-stage burn because of

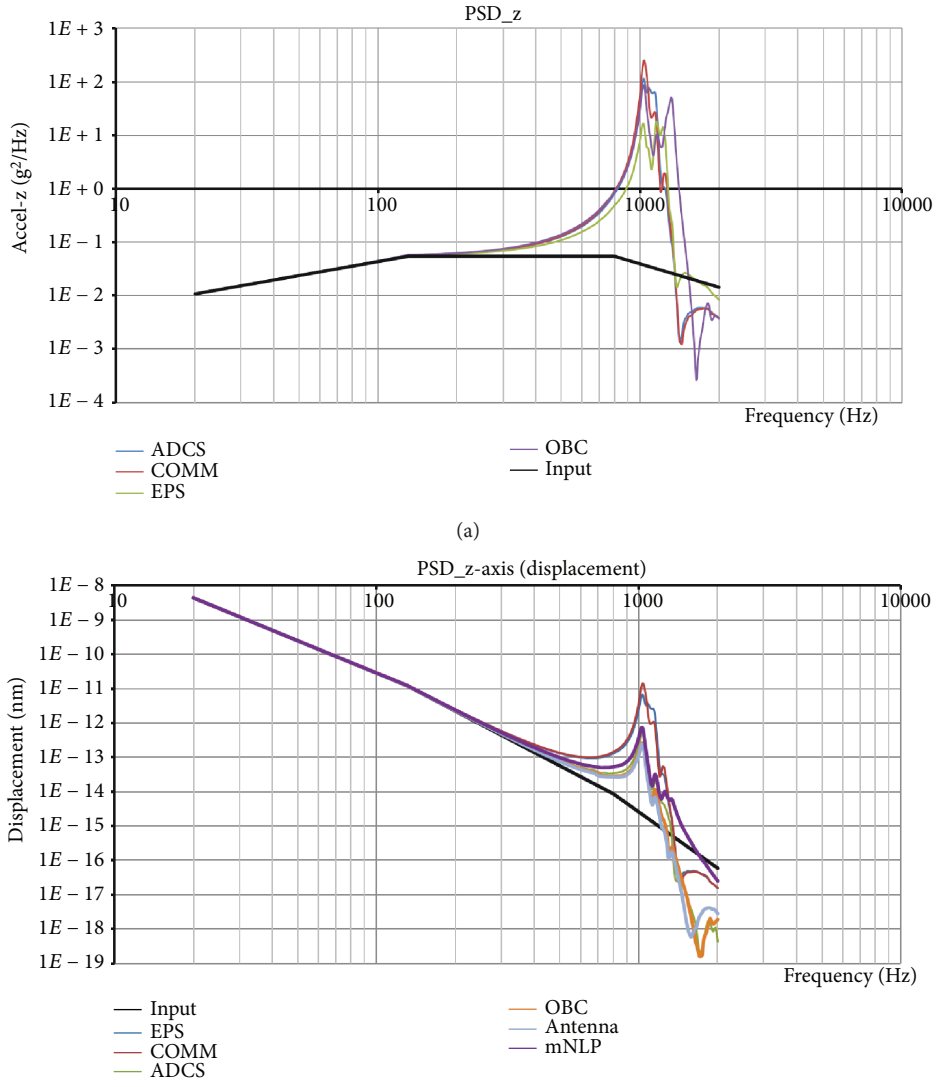

Figure 10: PSD results: (a) acceleration and (b) displacement.

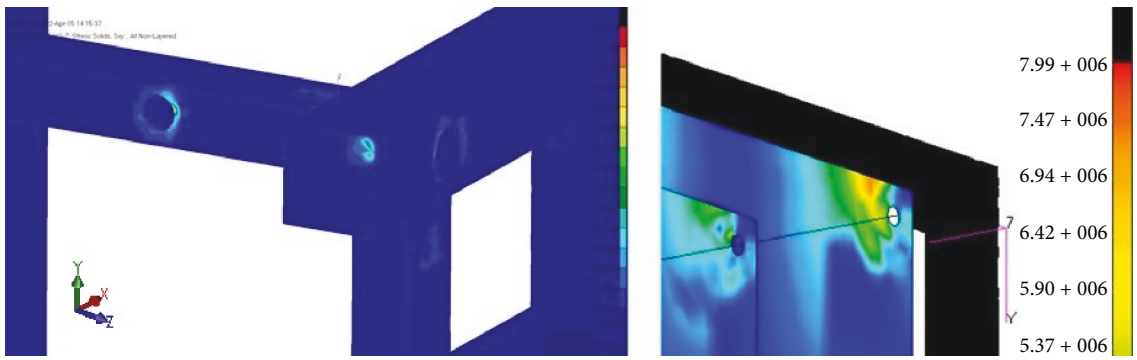

Figure 11: RMS stress distribution (PSD analysis).

the weaker mass of the launcher (the burned fuel mass being no longer present) for the same amount of thrust [15, 16]. Concerning the QB50 mission, the launch vehicle has already been identified [17], and thus for the worst loading case, a 13 g inertial load was applied at all three axes (three different loading scenarios).

Table 4: Orbit characteristics.

ISS orbit	
Semimajor axis (km)	6780
Eccentricity (degrees)	0
Ascending node longitude (degrees)	−94.354
Inclination (degrees)	51.64
Mean anomaly (degrees)	254.215

2.3.3. Vibrations. One of the most severe loads for the integrity of the cubesat structure (both internal and external) is the random vibrations coming from the spacecraft launch. The purpose of random vibration analysis is the verification of strength and structural integrity of the satellite by introducing random vibrations through the mechanical interface. This kind of analysis is best suited for subsystem/equipment-level tests and serves for the verification of the satellite structure [18].

The typical way to describe the severity of loading and the possible damage under random vibration is in terms of the application of the PSD (power spectral density) that the satellite will face during its own launching, a measure of vibration amplitude power intensity in the frequency domain (Figure 2). The way to evaluate the constantly changing acceleration amplitude is to determine the average value of all the amplitudes within a given frequency range. Although acceleration amplitude at a given frequency constantly changes, its average value tends to remain relatively constant.

Random vibration analysis is usually performed over a large range of frequencies: from 20 to 2000 Hz, in the case of the most microsatellites. Such a study does not look at a specific frequency or amplitude at a specific moment in time but rather statistically looks at the response of the structure to a given random vibration environment. Finally, the aim of the analysis is to know the overall response of the structure throughout the frequency range of interest [19, 20].

2.4. Cubesat Platform Finite Element Model. The design of the structure is given in Figure 3, in a configuration with both solid and surface parts. All the aluminum parts were modelled as solid parts, while the CFRP side faces and the PCBs were considered as surface parts. Then, the CAD design was inserted in the MSC PATRAN preprocessor and the meshing strategy applied. Shell elements (QUAD4 that defines isoparametric membrane bending quadrilateral plate elements with rotational degrees of freedom normal to the plate) were used for the discretization of all surface parts following the Paver mesher methodology. On the other hand, solid tetrahedral elements (Tet10) were used for the discretization of all solid parts. The concluded finite element model is shown in Figure 4.

All bolted connections were modelled using beam elements (RBE3 Interpolation Element; the interpolation elements allow to model the motion of one or more grid points as a function of the motion of the other points) offering multipoint constrains (MPCs) [21]. For these elements (Figure 5(a)), stainless steel properties were assigned.

Concerning the inner structure, all four PCBs (EPS (electrical power supply), ADCS (attitude determination and control system), OBC (on-board computer), and COMM (communication)) were modelled as surface parts and meshed as described before using QUAD4 elements and FR4 material (continuous filament-woven fiberglass sheets bonded with flame-resistant epoxy resin) properties were considered (Table 2). The PCBs connected with the aluminum square parts using 1D-Bar elements, as Figure 5(b) shows, simulating the Brass spacers. All other major components (the camera, the batteries, the antenna system, and the mNLP unit) were modelled as 0D lumped masses. This practice helped to save computational time, but it was at the cost of the accuracy of vibration response at the lower frequencies.

Finally, the boundary conditions (Figure 5(c)) were applied according to the position of the cubesat inside the separation Poly Picosat Orbital Deployer module; all four rails were considered fully clumped. P-POD [22] is the standard deployment system that carries the cubesat during the launch mission and set it in orbit.

Prior to any analysis, a connectivity check of the model was performed, and after that a detailed convergence study of the developed model was implemented. The final mesh used for the rest of the analysis fulfills both the aforementioned checks.

3. Verification by Analysis

In this section, the structural analysis of the UPSat 2U cubesat platform is presented. All necessary data concerning the launcher loads (quasistatic and random vibration) and operation loads (trajectory for thermal analysis) were taken from the QB50 mission requirements [23] and concern only this particular mission.

3.1. Modal Analysis Results. Figure 6 shows the first 4 eigenfrequencies together with the corresponding eigenmodes (bending modes) for the UPSat structure. The lower limit for the first eigenfrequency for the specific mission is set above 90 Hz. In the present analysis, the 1st eigenfrequency is close to 500 Hz and thus the structure can be considered adequately robust concerning its modal characteristics.

3.2. Quasistatic Analysis Results. For the current mission, an inertial load equal to 13 g was considered, along the 3 major axes under clamped boundary conditions, as it was earlier discussed. Table 3 summarizes the results of the quasistatic analysis performed for all loading cases. As the structure consists of both aluminum and composite parts, both von Mises and maximum principal stresses were calculated and reported along with the maximum displacements and strain for all cases.

As it is evident from the results, all maximum stresses and displacements for all cases are extremely low, considering the strength of both materials. This is expected, since the structure was designed on the basis of a stiffness-driven approach, in order to push eigenfrequencies to higher values. The stress and displacement distributions are shown in Figures 7 and 8, respectively, for the worst-case scenario

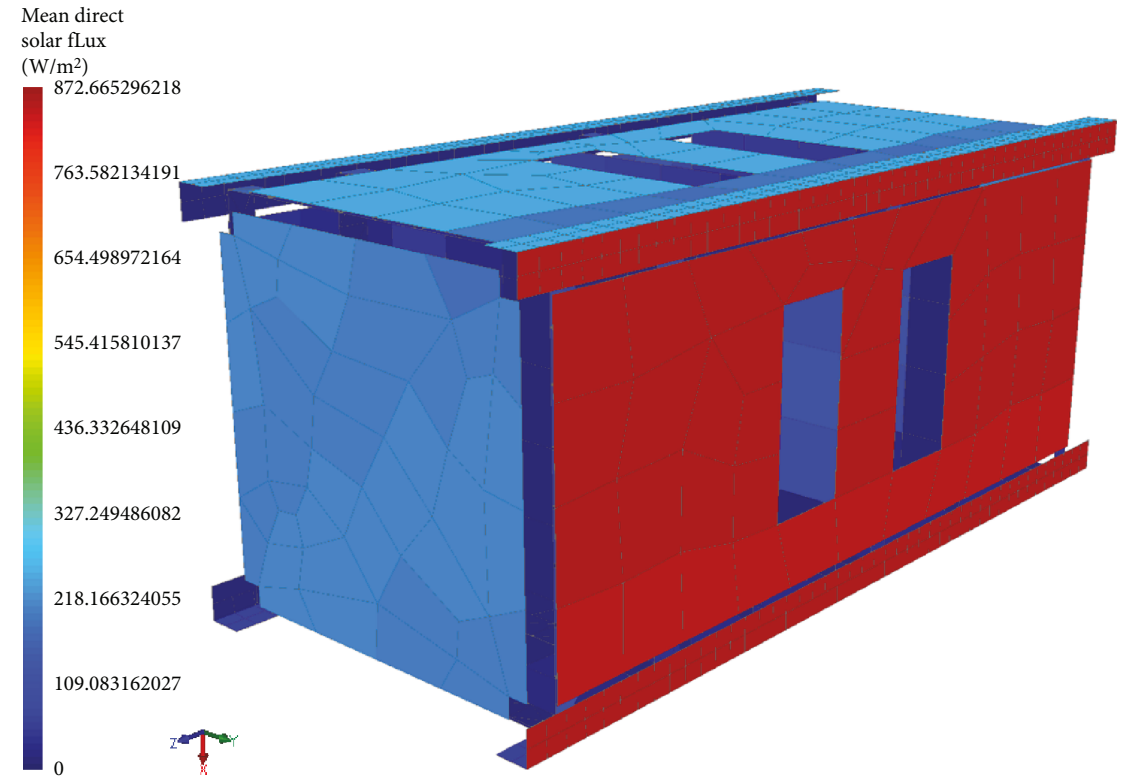

(a)

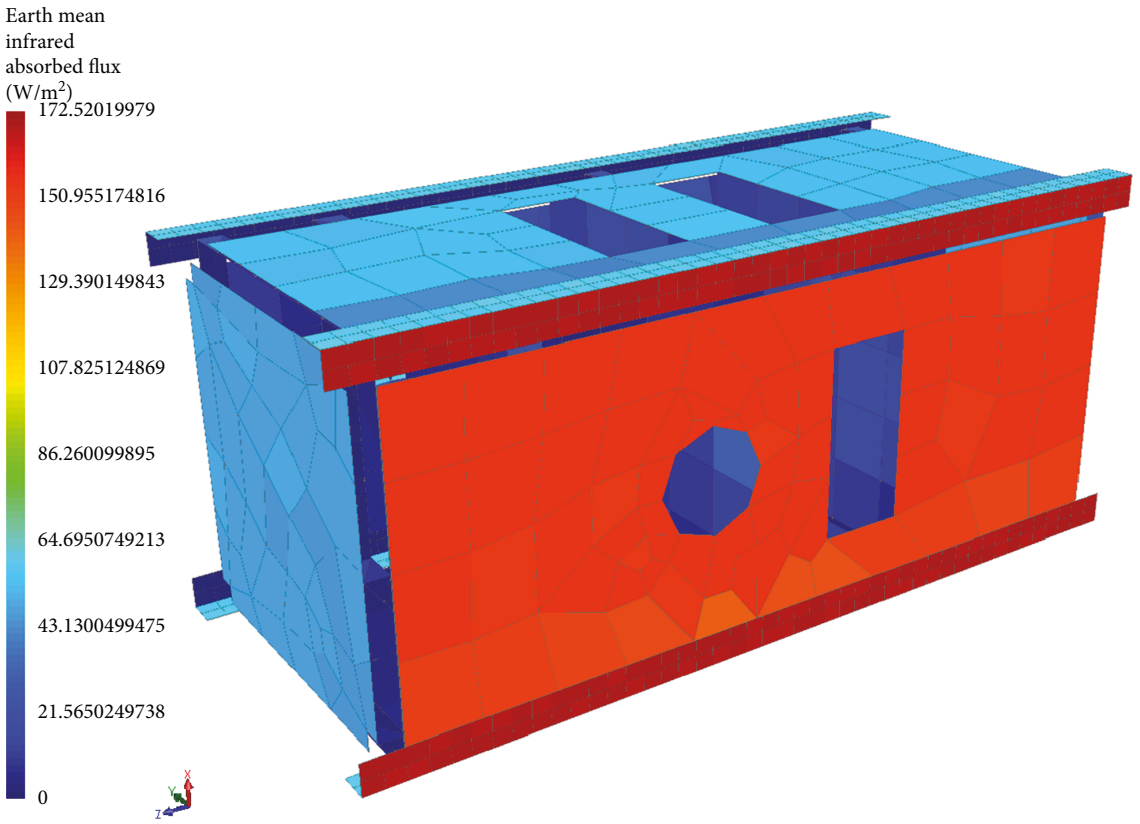

(b)

Figure 12: (a) Mean absorbed solar flux (872.66 W/m^2) and (b) mean absorbed Earth IR flux (172.52 W/m^2).

Table 5: Operational temperature limits.

Component	Operational temp limit (°C)
OBC (mother board)	−40 to +85
OBC (processor board)	−40 to +85
EPS	−40 to +85
Battery	−10 to +50
Magnetometer	−120 to +50
Sun sensor	−40 to +125
Solar cell	−100 to +65

Table 6: Maximum/minimum temperatures.

	Max temp (°C)	Min temp (°C)
Steady state	+26 (+Y face)	−38 (−Y face)
Transient state	+56 (+Y face)	−35 (−Y face)

(*x*-axis loading), and Figure 9 illustrates the stress distribution in the deformed structure, for the *z*-axis case.

Summarizing, the developed maximum stresses, displacements, and strains are very low, considering the strength of all materials used in the FE model. For example, the failure strain for the CFRPs is 1% (0.01) and the values for the strain at *x*- and *y*-loading cases are 10^{-5}, and thus the cubesat chassis, and therefore the entire system, can be considered adequately robust.

3.3. Random (PSD) Vibration. The input chart [frequency (Hz) versus amplitude (g^2/Hz)] presented in Figure 2 and the margin of safety (MoS = 0.25) were given by the project coordinator [23] and, similarly to the quasistatic analysis, should be applied at all the three axes of the coordinate system. Figure 10 illustrates the responses in g^2/Hz and displacement (mm) of the central node of each PCB versus frequency at the range up to 2000 Hz in the *z*-direction.

The square root of the area under the PSD curve (grey area) in Figure 2 gives the root mean square (RMS) value of the acceleration, or Grms, which is a qualitative measure of intensity of vibration. The maximum stress for all three scenarios was identified around the PCB holes (Figure 11 illustrates the stress distribution for the *z*-axis case).

Similar results are concluded for both the g^2/Hz and the displacement responses as well as for the RMS stress distribution when the input acceleration profile was applied on the *x*- and *y*-axes. All RMS stresses for the three scenarios of PSD analysis are extremely low and not capable of raising any concerns regarding the structure's integrity.

3.4. Orbital Case: Thermal Analysis. As the cubesat will be deployed from the International Space Station, the trajectory of ISS was considered for the thermal analysis. This trajectory is a low-Earth orbit with the characteristics given in Table 4.

The FE model was presented earlier for the mechanical analysis, simplified according to the needs of the Thermal Analysis software (MSC Thermica) and all the necessary covers and coatings (MLI, solar cell, etc.) included. Figure 12 presents the mean absorbed solar flux and the mean absorbed Earth IR flux applied into the cubesat structure.

The next step was the calculation of the temperature distribution for the entire cubesat system. The results for both the steady-state and transient state analyses are presented in Table 5. Both maximum and minimum temperatures were noticed at the outer faces of the cubesat while the temperatures for all internal electronic subsystems were inside the permitted limits for normal operation (Table 6). For example, the maximum/minimum temperatures noticed on the EPS system, during the transient state analysis, were +28°C/+2°C.

4. Cubesat Verification Tests

4.1. Manufacturing and Assembly. The development of all UPSat subsystems took place at AML/UPAT and LSF facilities following a non-COTS component philosophy, and the final assembly and integration were performed inside a clean room area (ISO-7) following all recommendations described in [24].

Concerning the manufacturing of CFRP sides, the space-approved composite material HTM143/M55J (6K) Cyanate-Ester/Carbon unidirectional pre-preg (CYTEC manufacturer) was selected as a material that was previously used in a flight-proven aerospace structure [25]. The standard pre-preg autoclave procedure was followed, and the entire process was completed at AML/UPAT facilities.

The assembly and integration (system level) of the 2U cubesat is illustrated in Figure 13, showing on the right the actual flight model, ready for the testing campaigns. The total mass of the flight model was found at 1.75 kg, meaning that there was almost a kilogram available for use of any extra scientific instrumentation (max allowable mass of a 2U cubesat is 2.66 kg).

4.2. Testing Campaigns. For the need of the vibration campaign, an intermediate structure is required. The test pod simulates the actual boundary conditions that the cubesat will experience during launch, and it is necessary to be as rigid as possible for transferring the vibration loads from the shaker table to the cubesat without any resonances. The test pod, made of aluminum alloy (7075), was designed and manufactured in-house and passed all design (cubesat fit check) and test criteria (no resonance below 90 Hz).

The experimental setup shown in Figure 14 is the same for all required vibration tests (resonance, quasistatic, random, and sine vibration). For the *x*- and *y*-axis loading cases, the right setup was used and the cubesat rotated 90 degrees inside the test pod. For the *z*-axis case, the entire system (cubesat and test pod) was rotated and the left setup was used. The vibration campaign was performed at the Hellenic Aerospace Industry (HAI) facilities, and two different campaigns were completed: a qualification campaign using several dummy masses (solar panels, camera) and QM models for the PCBs and an acceptance campaign using the actual flight model of the fully assembled cubesat.

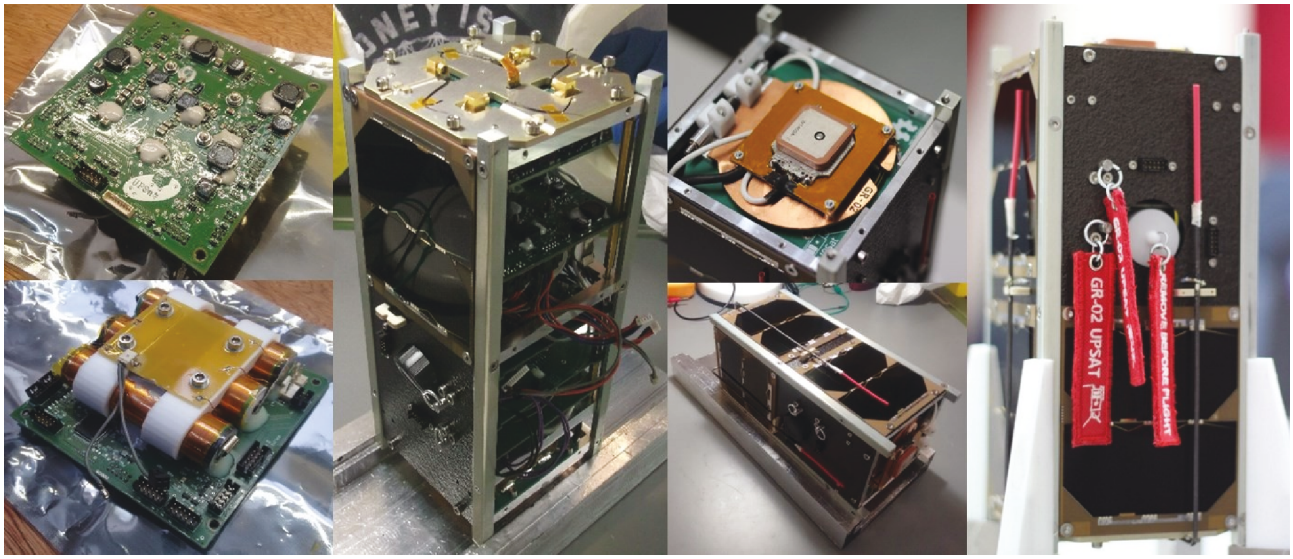

Figure 13: Assembly and integration procedure of UPSAT.

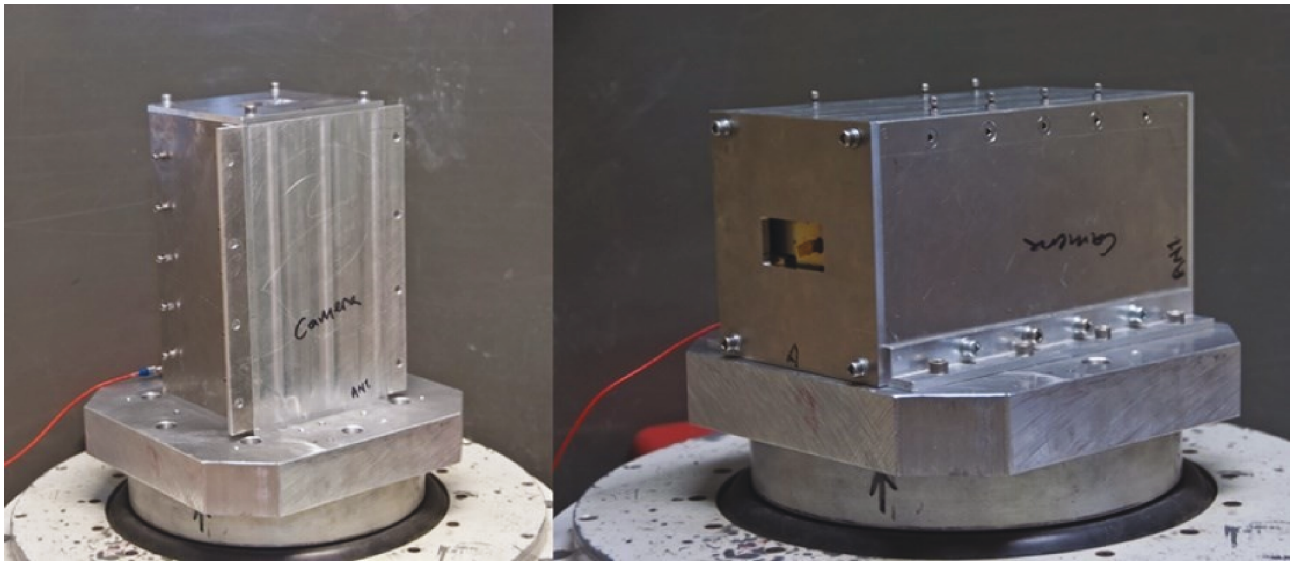

Figure 14: Vibration campaign test setup.

The first and most important test during the vibration campaign is the resonance survey test. The resonance survey serves as reference for the entire campaign, as this test is performed before and after a test at full level for each axis (quasistatic, sine, and random). By comparing the results of the resonance survey tests, a change in cubesat integrity due to settling or possible damage can be predicted.

The resonance frequency test is the experimental way to verify that the assembled system's natural frequencies are within the specification limits. According to QB50 functional specifications [11], the required frequency profile is from 5 to 100 Hz, in order to verify that the structures' lowest natural frequency is above 90 Hz. The variation of natural frequencies before and after each axis test at full level is the actual test pass criterion for the vibration campaign.

In our case, this variation was found to be no more than 1% for all three loading scenarios. Although similar responses were recorded for all cases, only the results for the z-axis are presented here, as this case was of greater interest, due to the changes at the experimental setup: a 90-degree rotation of test fixture. The detailed results of all loading cases of the campaign are presented in [26].

Figure 15 illustrates the system's response for the z-axis case (PSD vibration) and Figure 16 the variation on resonance test (before and after full level) for the same case. The spike at frequencies below 100 Hz is attributed to the vibration table setup; the same spike was noticed during the test of the test pod (without the cubesat inside) and also during the standalone test of the table setup prior to any other test.

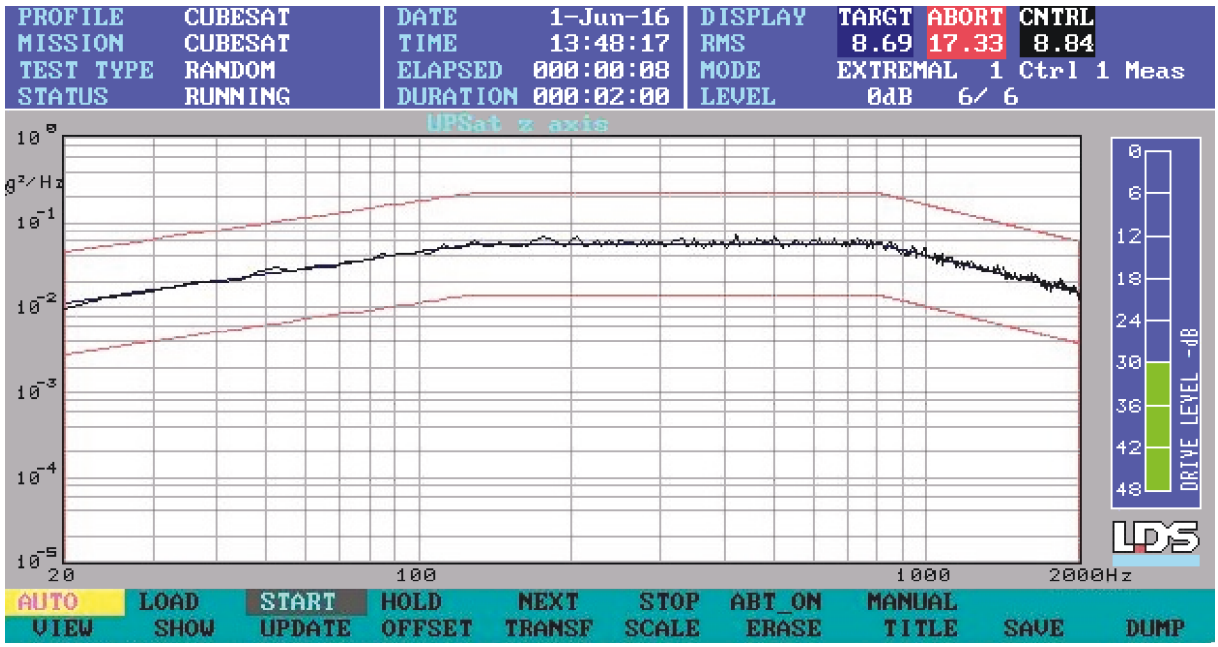

Figure 15: PSD response (z-axis).

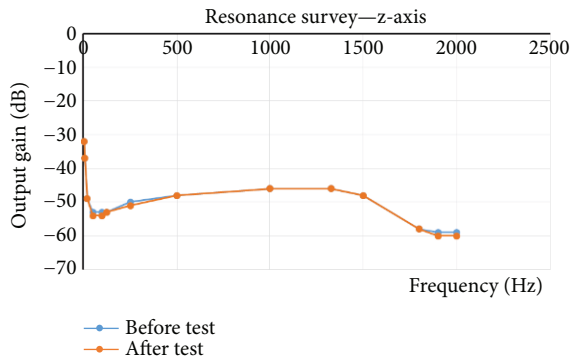

Figure 16: z-axis response and resonance test.

Using the resonance survey results, visual inspection on the satellite after each full cycle, and a short reference functional testing campaign after all full cycles, the vibration campaign was deemed as successful and the T-VAC campaign started.

The thermal testing campaign requires a thermal vacuum chamber, capable of offering the necessary vacuum and thermal/cooling conditions for the needs of required tests. Such a chamber is designed and manufactured in-house (AML), following the literature survey [27], and is presented in Figure 17. The T-VAC setup offers vacuum up to 10^{-1} mbar, controlled heating up to 60°C (halogen lamp), and controlled cooling by a cooling coil up to −40°C (R404 cooling agent). Finally, 6 temperature sensors were used for control and monitoring as Table 7 shows.

The two different tests required by [23] are the thermal cycling and the thermal bake-out. During the thermal cycling test, the cubesat was subjected in 4 thermal cycles (−20°C to +50°C) and remained for one hour at the extreme temperatures (after TC-6 and then TC-1, indicating temperature stabilization). The cubesat was fully functional and operational as several functional tests had to be performed (as specified in [11]).

On the other hand, during the thermal bake-out test, the satellite is not operational as the success criterion of this test is the total mass loss of the satellite. The total outgassing of the materials from all subsystems should not exceed 1% of the total mass of the satellite.

The thermocouples' response is illustrated in Figure 18(a) showing the experiment's four cycles from −20°C to +50°C and finally the cooling down to room temperature (25°C). The total test duration was 7 hours, and the only malfunction during the test was a sudden shutdown of the halogen lamp for 5 seconds, which caused the sharp temperature drop (TC-2, TC-3, and TC-4) shown in Figure 18. The temperatures on the PCBs during the test never reached values of high risk, and all required functional tests performed during the plateaus did not indicate any malfunction on any of the PCBs. Some of the completed functional tests are shown in Figure 18(b).

The test duration of the thermal bake-out test was increased to 24 hours, instead of 3 hours (after the coordinator's suggestion), due to low vacuum inside the chamber (the desired vacuum was 10^{-5} mbar). The satellite's weight before (1753.5 grams) and after (1752.7 grams) the test offered a total mass loss close to 0.045% (should be <1% by requirements).

After the successful completion of both testing campaigns, the flight readiness phase concluded successfully and the cubesat was ready for shipment. The cubesat was delivered to ISISpace in Delft on the 18th of August 2016 for the check-out process, which included several health checks on the satellite, the fit check inside a dummy POD,

Figure 17: Thermal vacuum chamber (setup and internal view).

Table 7: Position of temperature sensors.

TC-1	+Y (control)
TC-2	+X
TC-3	−X
TC-4	+Y (zenith—sun face)
TC-5	−Y (nadir—earth face)
TC-6	Attachment frame (control)

and full charging of the batteries. The integration on NanoRacks deployers took place on the 22nd of November (Figure 19(a)) and the deployers were delivered to Orbital ATK, for the final integration into the Cygnus CRS OA-7 cargo and then atop the Atlas V launcher on February 14th (Figures 19(c) and 19(d)).

The launch, from Cape Canaveral, took place on 18th of April, and the Cygnus cargo berthed successfully on ISS on the 22nd of April (Figure 19(d)). Finally, UPSat was deployed from ISS, on May 18th (Figure 19(e)), and after one hour, successful contact with UPSat was achieved, with the received CW beacon and Whole Orbit Data (WOD) verifying the perfect condition of the cubesat and thus the mission success. Currently, attempts for commissioning from the local ground segment are ongoing.

5. Conclusions

In this study, the structural design optimization and development of a 2U cubesat were investigated. The goal of the study was to design, build, and verify by analysis and test a "hybrid" cubesat structure while attempting to quantify the benefits for such a choice.

The first and most important conclusion from the current work was that a successful design optimization and verification by analysis of a 2U cubesat was one using a novel hybrid composite structure which could bring significant mass savings. The UPSat structure offered a first frequency higher than the lower limit required (90 Hz). Furthermore, a reduction of mass close to 30% was attained between the "hybrid" structure and a full aluminum one, leading to an overall lighter cubesat system. This means that using composite materials and after evaluation for the moat optimum design and proper lamination, the structure could be more stiff and lighter than a conventional aluminum cubesat structure. This reduction could allow adding an extra payload and expanding the mission's objectives; this was one of the team's goals during the preliminary design review phase. For the 2U cubesat analyzed, the overall mass savings in the platform design allowed for a 1 kg payload mass available. Unfortunately, by the end of the critical design review phase, such a payload was not available, and the system design concluded with a 34% free mass budget.

All types of analysis (quasistatic, PSD, and thermal) gave also quite satisfactory results, and no need for redesign occurred during the critical design review phase of the project.

The proposed design was manufactured, fulfilling the required cubesat design tolerances, and the fully assembled cubesat system was subjected to all required tests according to mission specifications. Both vibration and T-VAC campaigns were completed successfully, and for all subsystems, the normal operation before, during, and after the tests was verified, thus making the cubesat flight ready.

The UPSat cubesat was delivered and integrated into the Atlas V launcher and set successfully into orbit fulfilling its main mission objective by returning successful housekeeping in orbit data. The CW beacon and WOD files confirmed the normal operation of all subsystems and make UPSat the first Greek open-source, designed-from-scratch, nanosatellite ever launched.

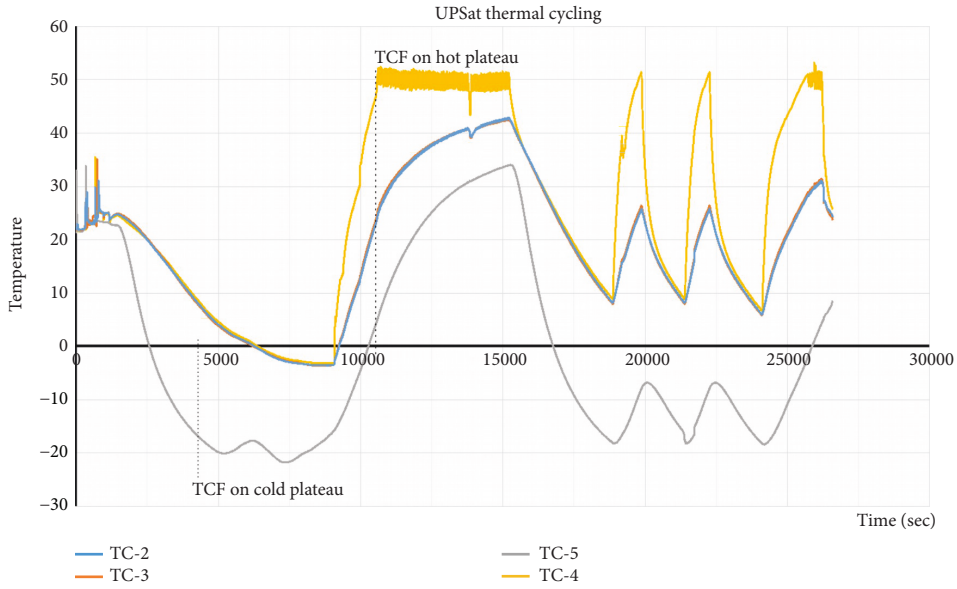

(a)

Subsystem	Test ID	Expected result	Actual result	Status (successful, failed, N.A.)	Note (if failed or not tested, reference of NCR or RfW)
OBC	OBC04	MS01	MS01	Successful	Read mass storage through MS service
	OBC06	WOD	WOD	Successful	Reception and decoding of WOD through RF
COMM	COM02	TS05	TS05	Successful	Test packet from UMB with GND destination
	COM03	TS06	TS06	Successful	Test packet from GND with UMB destination
EPS	EPS05	WOD	WOD	Successful	Reception and decoding of WOD through RF
	EPS08	5V	Sun Sensor ON	Successful	Sun Sensor is operating on +5V. ADCS DBG packets showed it works.
ADCS	ACS01	TS04	TS04	Successful	Test packet to ADCS and response

(b)

Figure 18: (a) Thermal cycling TC response (temperatures monitoring) and (b) some of the reference tests during thermal cycling.

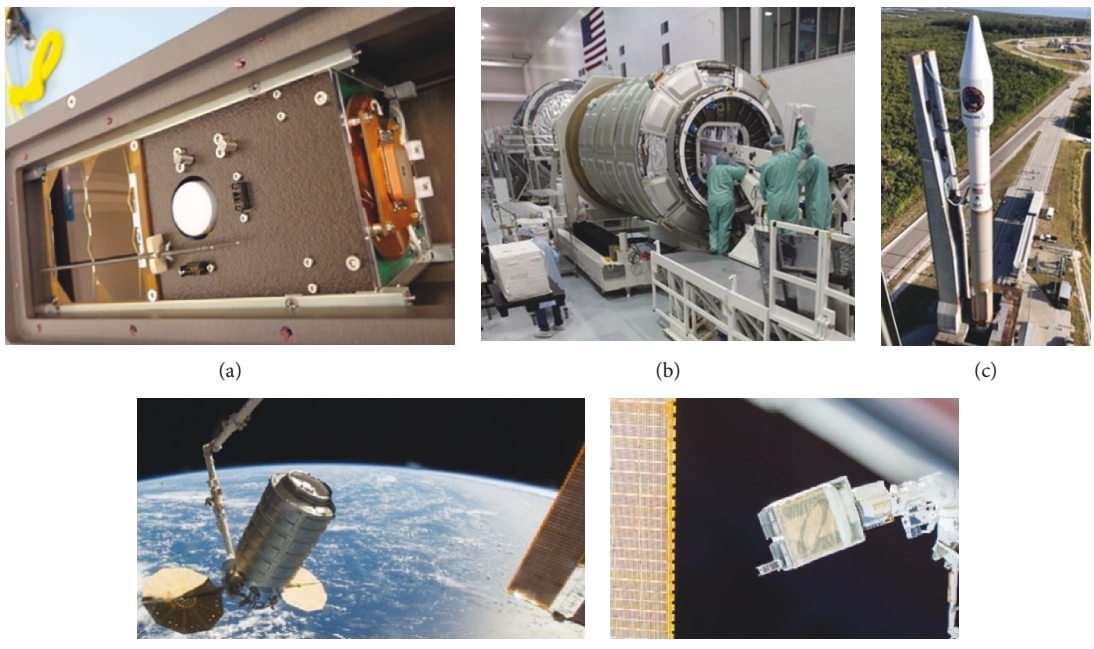

(a) (b) (c)

(d) (e)

Figure 19: (a) UPSat inside the NanoRacks deployers, (b) integration into the Cygnus cargo, (c) ready for launch, (d) cargo berthed on ISS, and (e) UPSat deployment from ISS.

Conflicts of Interest

The authors declare that there is no conflict of interest regarding the publication of this paper.

Acknowledgments

The authors would like to thank Dr. George Sotiriadis for his support in the manufacturing of the TVAC chamber.

References

[1] J. Puig-Sauri and R. J. Twiggs, *CUBESAT: Design Specifications Document, Revision III*, California Polytechnic State University and Stanford University's Space Systems Development Laboratory, 2005.

[2] W. J. Larson and J. R. Wertz, *Space Mission Analysis and Design*, Microcosm Press, 1999.

[3] T. P. Sarafin and W. J. Larson, *Spacecraft Structures and Mechanisms from Concept to Launch*, Microcosm, Inc., 1995.

[4] *ECSS-E-ST-32-08C–Space Engineering-Materials*, ESA Publications Division ESTEC, The Netherlands, 2008.

[5] *ECSS-E-ST-32C Rev. 1 – Structural General Requirements*, ESA Publications Division ESTEC, The Netherlands, 2008.

[6] D. Selva and D. Krejci, "A survey and assessment of the capabilities of cubesats for Earth observation," *Acta Astronautica*, vol. 74, pp. 50–68, 2012.

[7] A. Toorian, K. Diaz, and S. Lee, "The cubesat approach to space access," in *2008 IEEE Aerospace Conference*, pp. 1–14, Big Sky, MT, USA, 2008.

[8] H. Bansemir and O. Haider, "Fibre composite structures for space applications—recent and future developments," *Cryogenics*, vol. 38, no. 1, pp. 51–59, 1998.

[9] A. Diana, J. Benjamin, and R. Guillaume, *Design of a Swiss Cube Structure and Configuration*, LMAF, EPFL, Lausanne, Switzerland, 2006.

[10] A. Ampatzoglou, A. Baltopoulos, A. Vavouliotis, A. Kotzakolios, and V. Kostopoulos, *IAC-10.B4.6B.2 - Design and Analysis of a Full Composite Structure for the 1st Greek Cubesat by the University of Patras (UPSat)*, 61st International Astronautical Congress, Prague, Czech Republic, 2010.

[11] A. Ampatzoglou, A. Baltopoulos, A. Kotzakolios, and V. Kostopoulos, "Qualification of composite structure for cubesat picosatellites as a demonstration for small satellite elements," *International Journal of Aeronautical Science & Aerospace Research*, vol. 7, no. 1, pp. 1–10, 2014.

[12] ECSS Secretariat, *ECSS-E-ST-32-03C – Space Engineering: Structural Finite Element Models*, ESA-ESTEC, The Netherlands, 2008.

[13] European Space Agency and M. Appolloni, *Final YGT Report – Structure*, European Space Agency, 2004.

[14] "ECSS-E-ST-32 – Space engineering: structural general requirements".

[15] P. Fortescue, J. Stark, and G. Swinerd, *Spacecraft Systems Engineering*, John Wiley & Sons Ltd, 3rd edition, 2003.

[16] B. Mathieu, *OUTFI-1 Nanosatellite: Dynamic Analysis and Qualification Testing, [M.S. thesis]*, University of Liege, Faculty of Applied Sciences, 2011, Academic Year 2010–2011.

[17] "QB50, an FP-7 Project, QB50 Launch Scenario," 2012, https://www.qb50.eu/index.php/project-description-obj.

[18] A. Calvi, *Spacecraft Structural Dynamics & Loads: an Overview*, 2010, http://www.ltas-vis.ulg.ac.be/cmsms/uploads/File/CALVI—LIEGE_2010_Students.pdf.

[19] S. Kumar, "Analyzing random vibration fatigue: tips and tricks," *ANSYS Advantage*, vol. 2, no. 3, 2008.

[20] S. Tao, B. Chen, and X.-J. Fan, "Structural fatigue life prediction based on ANSYS random vibration analysis," in *Proceedings of the 4th 2016 International Conference on Material Science and Engineering (ICMSE 2016)*, pp. 235-236, Indonesia, 2016.

[21] "PATRAN/NASTRAN 2005 Documentation".

[22] "ISISPOD cubesat Deployer Specifications v7.11".

[23] "Amandine Denis, QB50 Systems Requirements and Recommendations (Issue 7)," 2015, February 2003, https://www.qb50.eu/index.php/tech-docs/category/25-up-to-date-docs.html.

[24] "Cubesat Integration (CI) Document".

[25] V. J. Lappas, *Surrey Space Centre Presented the GSF Keynote: Gossamer Systems for Satellite Deorbiting: the CubeSail and DeorbitSail Space Missions*, AIAA SDM, Honolulu, Hawaii, 2012.

[26] A. Ampatzoglou, *Design, Analysis and Optimization of a Micro-Satellite for the Study of Lower Thermosphere and Re-Entry conditions, [Ph.D. thesis]*, 2017, http://nemertes.lis.upatras.gr/jspui/bitstream/10889/10553/3/Nemertes_Ampatzoglou%28aer%29.pdf.

[27] S. Jayaram and E. Gonzalez, "Design and construction of a low-cost economical thermal vacuum chamber for spacecraft environmental testing," *Journal of Engineering, Design and Technology*, vol. 9, no. 1, pp. 47–62, 2011.